Planet. Space Sci., Vol. 41, No. 1, pp. 35–43, 1993
Printed in Great Britain.

0032–0633/93 $6.00+0.00

A two-dimensional model of the plasmasphere: refilling time constants

Craig E. Rasmussen, Steven M. Guiter and Steven G. Thomas

Space Physics Research Laboratory, Department of Atmospheric, Oceanic and Space Science, University of Michigan, Ann Arbor, MI 48109-2143, U.S.A.

Received in final form 23 July 1992

Abstract. A two-dimensional model of the plasmasphere has been developed to study the temporal evolution of plasma density in the equatorial plane of the magnetosphere. This model includes the supply and loss of hydrogen ions due to ionosphere–magnetosphere coupling as well as the effects of $\mathbf{E} \times \mathbf{B}$ convection. A parametric model describing the required coupling fluxes has been developed which utilizes empirical models of the neutral atmosphere, the ionosphere and the saturated plasmasphere. The plasmaspheric model has been used to examine the time it takes for the plasmasphere to refill after it has been depleted by a magnetic storm. The time it takes for the plasmasphere to reach 90% of its equilibrium level ranges from 3 days at $L = 3$ during solar minimum to as high as 100 days at $L = 5$ during solar maximum. Refilling is also dependent on the month of the year, with refilling requiring a longer period of time at solar maximum during June than during December for $L > 3.2$.

1. Introduction

The plasmasphere and, in particular, the shape of the plasmapause in the equatorial plane of the magnetosphere has been investigated by numerous workers (e.g. Carpenter, 1966; Binsack, 1967; Taylor *et al.*, 1968; Chappell, 1972; Maynard and Grebowsky, 1977). In general, these studies indicate a bulge in the evening sector location of the plasmapause and a decrease in plasmapause radius L with increasing geomagnetic activity. In addition to this general morphology, detailed structures in plasma density have also been found. Chappell (1974) noted the formation of detached regions of high-density plasma, while Ho and Carpenter (1976) suggested that these regions may actually be plasmaspheric tails or streamers which remain connected to the main body of the plasmasphere.

Plasmaspheric densities and the formation of the plasmapause are influenced by two primary effects: (1) a relatively uniform plasma source (the ionosphere) and (2) plasma transport which affects both the volume of a flux tube element and the amount of time a flux tube remains connected to the ionosphere before venting to interplanetary space. Hydrodynamic models of these processes have historically solved for plasma density, flow velocity and energy along a magnetic flux tube (e.g. Richards and Torr, 1985; Moffett *et al.*, 1989). These one-dimensional models can be used to follow the motion of several flux tubes, starting at varying initial L-values, in order to create a three-dimensional picture of the plasmasphere (Rasmussen and Schunk, 1990). However, this is not often done, as studies of this type require a significant amount of computer resources. For instance, because of the relatively long time scales for plasmasphere refilling, we have found that several hours of supercomputer time can be required just to reach equilibrium at a single L-shell.

For some types of plasmaspheric studies, including those considering plasmapause formation and the detachment of plasmaspheric tails, complete information along a flux tube is not required. Considerable simplification can be made by integrating the continuity equation along a flux tube from ionosphere to conjugate ionosphere. In this manner, a conservation equation for the total content of a flux tube can be obtained. This method for modeling the transport of thermal plasma in the equatorial plane of the magnetosphere was pioneered several years ago by Chen and Wolf (1972), but has largely been ignored since that time.

A total tube content model for the plasmasphere is particularly useful in studying the changes in plasmaspheric density brought about by variations in magnetospheric convection. For instance, as plasma is advected away from the Earth in the afternoon sector of the magnetosphere, the volume of a flux tube increases, and this brings about a corresponding decrease in plasma density. In many instances, the convection electric field causes a more rapid variation in density than does any other process. Time scales for advective changes in density can be of the order of 1 h or less. This compares to time scales for refilling which are of the order of a few days or longer.

Fluxes of particles entering (or leaving) the plasma-

Correspondence to: C. E. Rasmussen

sphere from conjugate ionospheres are the only way in which the total tube content can change. The maximum flux of plasma upwelling from conjugate ionospheres occurs when the plasmasphere is empty. These fluxes are relatively well understood, and analytical approximations for them have been developed (e.g. Richards and Torr, 1985). However, as the flux tube reaches saturation, these maximum fluxes are greatly reduced. Thus, in order to completely specify a total tube content model, a knowledge of ionospheric–magnetosphere coupling fluxes is required. One of the principal motivations for this study has been to find a way to parameterize the coupling fluxes in order to reduce the significant computer costs of a first-principles model of the fluxes.

In this brief note we consider the two-dimensional model of Chen and Wolf (1972) and suggest various improvements. In particular, a parametric model specifying the required ionosphere–magnetosphere fluxes is given. This is done in the next section, where we also examine the theoretical basis for the model and compare it with a complete field-line model in order to determine the relative accuracy of the total tube content model. We then use the model to make comparisons with measurements of plasmasphere refilling during periods of low magnetic activity. We also model the dependence of refilling rates on L-shell, on solar activity and on the month of the year.

2. Theory

In this section, the theoretical foundation of the two-dimensional model of the plasmasphere is given. The dominant mechanism for the production and loss of thermal H^+ is the charge exchange reaction, $O^+ + H \rightleftharpoons H^+ + O$. This reaction occurs primarily in the ionosphere and, thus, local production and loss of H^+ in the plasmasphere is negligible in comparison with the transport of ions to and from the ionosphere along field lines. Thus, an equation describing the conservation of the total number of ions in a flux tube can be derived by integrating the continuity equation along a field line and assuming that $\partial B/\partial t = 0$. The conservation equation is:

$$\frac{D_\perp N}{Dt} \equiv \left(\frac{\partial}{\partial t} + \mathbf{u}_\perp \cdot \nabla\right) N = \frac{F_N + F_S}{B_i}, \tag{1}$$

where:

$$N = \int \frac{n}{B} h_s \, ds \tag{2}$$

is total ion content per unit magnetic flux, n is H^+ density, t is time and $\mathbf{u}_\perp$ is the drift velocity perpendicular to the magnetic field. B_i is the magnetic field at the conjugate ionospheres and is inversely proportional to the cross-sectional area of a flux tube at the ionosphere. A dipole system is assumed with curvilinear coordinates (ϕ, q, s), where ϕ is azimuthal angle, s is aligned with the magnetic field and q is perpendicular to the other two coordinates and directed toward the Earth; h_s is the scale factor for s (see Appendix for a more complete description of the dipole coordinate system). Equation (1) was originally given by Chen and Wolf (1972) and explicitly states that the total content of a flux tube is constant, except for the contribution of fluxes F_N and F_S (positive upward) which leak in or out of the tube at the northern and southern ionospheres, respectively.

Expressing the convection velocity as:

$$\mathbf{u}_\perp = -\frac{h_q}{L^2}\frac{dL}{dt}\hat{\mathbf{e}}_q + h_\phi \frac{d\phi}{dt}\hat{\mathbf{e}}_\phi, \tag{3}$$

we obtain:

$$\frac{\partial N}{\partial t} + \frac{dL}{dt}\frac{\partial N}{\partial L} + \frac{d\phi}{dt}\frac{\partial N}{\partial \phi} = \frac{F_N + F_S}{B_i}, \tag{4}$$

where h_q and h_ϕ are coordinate scale factors, $\hat{\mathbf{e}}_q$ and $\hat{\mathbf{e}}_\phi$ are unit vectors and L is the McIlwain parameter (see Appendix for further details). Note that it has been assumed that dL/dt and $d\phi/dt$ are independent of s.

Total tube content N is not particularly useful if model results are to be compared with satellite data. Therefore, an average density:

$$\bar{n} = \frac{\int (nh_s/B)\, ds}{\int (h_s/B)\, ds}, \tag{5}$$

is defined. Finally, an equation for the evolution of average plasma density in a flux tube is obtained from equation (4):

$$\frac{\partial \bar{n}}{\partial t} + \frac{dL}{dt}\frac{\partial \bar{n}}{\partial L} + \frac{d\phi}{dt}\frac{\partial \bar{n}}{\partial \phi} = \frac{F_N + F_S}{B_i V} - \frac{\bar{n}}{V}\frac{dL}{dt}\frac{dV}{dL}, \tag{6}$$

where:

$$V(L) = \int \frac{h_s}{B}\, ds \tag{7}$$

is the volume per unit magnetic flux of a tube of plasma. To obtain equation (6), it has been assumed that B is independent of time and azimuthal angle ϕ. A question arises as to the relationship between the average density $\bar{n}$ and the plasma density, n_{eq}, near the equatorial plane of the magnetosphere. We show below that $\bar{n} = n_{eq}$ to a close approximation under most circumstances. Thus, it is suggested that equation (6) can be used effectively to model plasmaspheric density in the equatorial plane as long as ionospheric fluxes supplying the plasmasphere are known or can be approximated.

2.1. *Comparison of* $\bar{n}$ *and* n_{eq}

Because the tube content model does not solve for density variations along a field line, an important question to consider is how well plasma densities at the equator are approximated by the average density $\bar{n}$. Since the volume of a flux tube is dominated by contributions near the equatorial plane (here the magnetic field is lower and, consequently, the flux tube area is largest), a logical assumption is that $\bar{n} \simeq n_{eq}$. In this section we derive a

hydrostatic equilibrium solution which pertains to dipole field lines in order to consider this question.

Neglecting collisions, the momentum equation for plasma $\mathbf{E}\times\mathbf{B}$ convecting in a strong magnetic field is:

$$\left(\frac{\partial}{\partial t}+\mathbf{u}_\perp\cdot\nabla+\frac{u}{h_s}\frac{\partial}{\partial s}\right)u+\frac{1}{nmh_s}\frac{\partial}{\partial s}p_\parallel = \frac{(p_\parallel-p_\perp)}{nmBh_s}\frac{\partial B}{\partial s}+\boldsymbol{g}\cdot\hat{\mathbf{e}}_s+\frac{e}{m}E_\parallel + \mathbf{u}_\perp\cdot\left(\frac{\partial}{\partial t}+\mathbf{u}_\perp\cdot\nabla+\frac{u}{h_s}\frac{\partial}{\partial s}\right)\hat{\mathbf{e}}_s, \quad (8)$$

where $p_\parallel$ and $p_\perp$ are the parallel and perpendicular components of the pressure tensor, e/m is the charge to mass ratio, $E_\parallel$ is the ambipolar electric field, and $\boldsymbol{g}$ is the acceleration due to gravity (Gombosi and Rasmussen, 1991). The last term in equation (8) is an inertial force due to $\mathbf{E}\times\mathbf{B}$ drifts. In a dipole coordinate system this term is:

$$\mathbf{u}_\perp\cdot\left(\frac{\partial}{\partial t}+\mathbf{u}_\perp\cdot\nabla+\frac{u}{h_s}\frac{\partial}{\partial s}\right)\hat{\mathbf{e}}_s = -\tfrac{3}{2}r\sin\chi \times\left[\sin^2\theta\left(\frac{\mathrm{d}\phi}{\mathrm{d}t}\right)^2+\cos^2\chi(1+\cos^2\chi)\left(\frac{1}{L}\frac{\mathrm{d}L}{\mathrm{d}t}\right)^2\right] -\tfrac{3}{2}u\cos^2\chi(1+\cos^2\chi)\left(\frac{1}{L}\frac{\mathrm{d}L}{\mathrm{d}t}\right), \quad (9)$$

where θ is colatitude and χ is the inclination angle of the magnetic field from the horizontal (see Appendix).

An equilibrium solution can be found to equation (8) by assuming that the parallel velocity u is small compared to the ion thermal speed. Defining:

$$\xi = -\int_{s_0}^{s}\left[\frac{\boldsymbol{g}\cdot\hat{\mathbf{e}}_s+\mathbf{u}_\perp\cdot\left(\frac{\partial}{\partial t}+\mathbf{u}_\perp\cdot\nabla\right)\hat{\mathbf{e}}_s}{\mathrm{K}T_\parallel}\right]h_s\,\mathrm{d}s, \quad (10)$$

$$\Phi = -\int_{s_0}^{s}\frac{E_\parallel}{\mathrm{K}T_\parallel}h_s\,\mathrm{d}s \quad (11)$$

and:

$$\Lambda = \int_{s_0}^{s}\frac{(p_\parallel-p_\perp)}{p_\parallel B}\frac{\partial B}{\partial s}\,\mathrm{d}s, \quad (12)$$

where K is Boltzmann's constant, it can be shown that:

$$n(s) = n_0\frac{T_\parallel(s_0)}{T_\parallel(s)}\mathrm{e}^{-e\Phi}\mathrm{e}^{-m_i\xi}\mathrm{e}^{\Lambda}, \quad (13)$$

where s_0 is chosen in the region where H^+ is in chemical equilibrium. The equilibrium value for H^+ is:

$$n_0(\mathrm{H}^+) = n_0(\mathrm{O}^+)\frac{L_{\mathrm{O}^+}}{L_{\mathrm{H}^+}}, \quad (14)$$

where $L_{\mathrm{O}^+} = 2.5\times10^{-11}\,T_n^{1/2}n(\mathrm{H})$ is the O^+ loss rate, $L_{\mathrm{H}^+} = 2.2\times10^{-11}\,T_i^{1/2}n(\mathrm{O})$ is the H^+ loss rate, both at $s = s_0$, and T_n and T_i are the neutral and ion temperatures, respectively.

Equation (13) describes the equilibrium solution for either of the ions H^+ or O^+, or for the electrons n_e, as long as correct parameters such as the constituent charge and mass are chosen. Assuming charge neutrality, $n_e = n(\mathrm{H}^+)+n(\mathrm{O}^+)$, neglecting the contribution of electron mass, and considering only altitudes high enough so that $\exp(-15m_{\mathrm{H}^+}\xi) \ll L_{\mathrm{O}^+}/L_{\mathrm{H}^+}$ (roughly above 3000 km), it can be shown that plasmaspheric densities follow:

$$n(s) = n_0(\mathrm{O}^+)\left(\frac{L_{\mathrm{O}^+}T_{i\parallel}(s_0)}{L_{\mathrm{H}^+}T_{i\parallel}(s)}\right)^a\left(\frac{T_{e\parallel}(s_0)}{T_{e\parallel}(s)}\right)^{(1-a)} \times\mathrm{e}^{-am_i\xi}\,\mathrm{e}^{a\Lambda_i}\,\mathrm{e}^{(1-a)\Lambda_e}, \quad (15)$$

where the parameter $a = T_{i\parallel}(s)/[T_{e\parallel}(s)+T_{i\parallel}(s)]$ is assumed to be independent of s. In equation (15), the subscript e denotes electron quantities while subscript i denotes H^+ quantities. The approach taken above is similar to that of Li *et al.* (1983), except that equation (15) correctly takes into account pressure anisotropies. Note that if the neutral, electron and ion temperatures are approximately equal, then $a \simeq 1/2$ and saturated plasmaspheric densities are proportional to:

$$n_{\mathrm{sat}} \propto n_0(\mathrm{O}^+)\sqrt{L_{\mathrm{O}^+}/L_{\mathrm{H}^+}} \simeq n_0(\mathrm{O}^+)\sqrt{n_0(\mathrm{H})/n_0(\mathrm{O})}. \quad (16)$$

An analytical solution for the variation of plasma density along a dipole field line can be obtained from equation (15) if temperatures are constant and isotropic and inertial forces in equation (10) are neglected:

$$n(\theta) = n_{\mathrm{eq}}\exp\left(\frac{R_{\mathrm{E}}\cot^2\theta}{H_0 L}\right), \quad (17)$$

where n_{eq} is the equatorial density (at $\theta = \pi/2$), $H_0 = \mathrm{K}(T_i+T_e)/mg_0$ and g_0 is the acceleration of gravity at Earth's surface. Equation (17) is the standard hydrostatic density distribution (e.g. Rishbeth and Garriott, 1969), except that it is solved for a dipole field geometry. Although equation (17) may seem like a considerable oversimplification, it is often a very good approximation to the variation of plasmaspheric density along the field line. For instance, in Fig. 1, the hydrostatic distribution (*solid curve*) is compared with a numerical solution

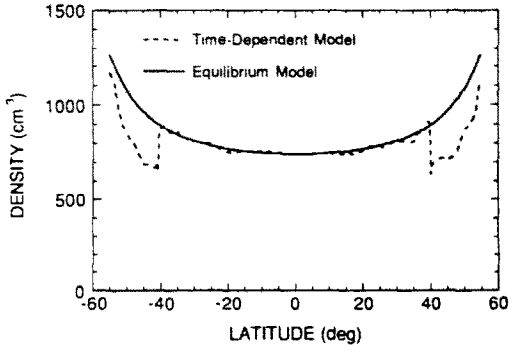

Fig. 1. A comparison of the hydrostatic equilibrium solution (*solid curve*) to a time-dependent numerical solution for refilling conditions. H^+ density and temperature in the hydrostatic solution [equation (17)] were matched to the numerical solution at the equator

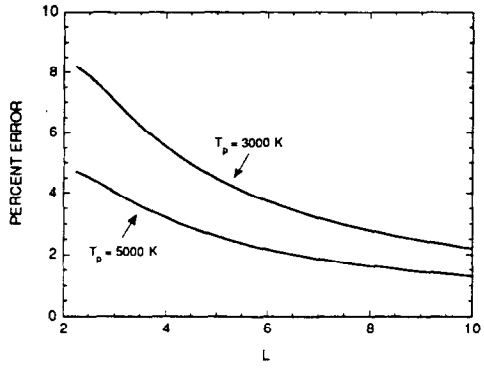

Fig. 2. The percentage error made by replacing the equator density n_{eq} with the average density $\bar{n}$. The error is given as a function of L-shell for two different temperatures $T_p = (T_i + T_e)/2$

(*dashed curve*) for similar conditions (constant and isotropic temperatures). Even for highly nonequilibrium conditions with shocked refilling flows, the hydrostatic distribution compares very favorably with the numerical solution in the equatorial region between -40° and 40° latitude.

We are interested in the ratio $n_{eq}/\bar{n}$, which is obtained by numerically integrating equation (17) along a field line to obtain the average density $\bar{n}$. The error, $1 - n_{eq}/\bar{n}$, is shown in Fig. 2 as a function of L for two temperature values. It is seen that $\bar{n}$ is very nearly equal to n_{eq}, with a maximum error of less than 10%. It should be noted, however, that during the early stages of refilling there may be a larger discrepancy between $\bar{n}$ and n_{eq}, particularly if shocked flow occurs (see Fig. 1) or if velocity distributions deviate significantly from a Maxwellian. Singh (1991) has used a refilling model which includes anisotropic temperatures to show that shocked flow and temperature anisotropies disappear within 5 h after flux tubes become severely depleted. Thus, during most of the time that refilling occurs, average tube content can be safely compared with measurements in the vicinity of the equatorial plane of the magnetosphere. It is only during the very early stages of refilling that density distributions along field lines deviate significantly from hydrostatic solutions of the form described by equation (17).

2.2. *Ionospheric fluxes*

The total tube content model is simply a statement that the number of ions in a flux tube remains constant, except for ions which enter or leave the tube at the ionospheric boundaries. Thus, much of the physics in the model lies in specifying the required ionospheric fluxes. One simple approximation is to assume that equilibrium densities are approached at a rate which depends on the variation from equilibrium and a time scale τ, i.e.:

$$\frac{F_N + F_S}{B_i V} = \sum_{s=N,S} \frac{n_s(L,\phi) - \bar{n}(L,\phi)}{\tau_s}, \tag{18}$$

where n_N and n_S are hemispheric equilibrium or saturation levels at the plasmaspheric equator, corresponding to the Northern (N) and Southern (S) Hemispheres, respectively. Equation (18) is similar to an equation derived by Krinberg and Tashchilin (1982), except that it can account for seasonal asymmetries and interhemispheric flows. Hemispheric saturation levels can be obtained from equation (15), or approximated from empirical models [such as the one recently developed from *ISEE* and whistler data (Carpenter and Anderson, 1992)].

Time scales:

$$\tau_s = \frac{n_s(L,\phi) B_i V}{F_{ls}}, \tag{19}$$

are obtained from equation (18) by assuming that the flux tube is completely empty ($\bar{n} = 0$); it is at this time when the upgoing ionospheric fluxes are at a maximum. These limiting fluxes are approximated by the analytical formula of Richards and Torr (1985):

$$F_l = L_{O^+} n(O^+) H(O^+), \tag{20}$$

where $H(O^+)$ is the oxygen ion scale height. The parameters in equation (20) should be calculated at the height z_0 where diffusion and loss terms in the continuity equation are equal. See Appendix B of Richards and Torr (1985) for a derivation of this height. Note that the constant 2×10^{19} in their formula (B9), should instead be 7.5×10^{18} (P. G. Richards, private communication, 1992). Neutral temperatures and densities required to calculate z_0 and the limiting fluxes are obtained from the MSIS-86 (Hedin, 1987) empirical model. The international reference ionosphere (IRI) model (Bilitza, 1986) is used to obtain ion and electron temperatures and O^+ density at 500 km. These parameters are then used to calculate the diffusion boundary altitude z_0, after which the same parameters are obtained at z_0 and used in equation (20) to obtain the limiting fluxes.

2.3. *Saturation density*

Equation (18) implies that upgoing ionospheric fluxes are maximized when the flux tubes are empty and decrease as the tubes fill with plasma. If the average tube density is greater than the equilibrium value, for instance at night, then equation (18) requires the existence of a downward flux which would deplete tube content (note that this assumes that refilling time scales are equal to emptying time scales). Indications of this process can be seen in Fig. 3, where O^+ (*solid lines*), H^+ (*short-dashed lines*) and chemical equilibrium H^+ (*long-dashed lines*) profiles are shown. The results were calculated with a numerical model which solves the time-dependent continuity, momentum and energy equations for O^+ and H^+ from 200 km in one ionosphere to 200 km in the conjugate ionosphere (Guiter *et al.*, 1991). The conditions in Fig. 3a represent the summer Northern Hemisphere ($L = 2$) at 12:00 L.T., and in Fig. 3b at 24:00 L.T. Even though H^+ levels (*short-dashed line*) in Fig. 3a were calculated for a "full" flux tube (the model was run until diurnally reproducible results were obtained), the H^+ valley near 1000 km is the classic signature of substantial upgoing fluxes near the limiting level.

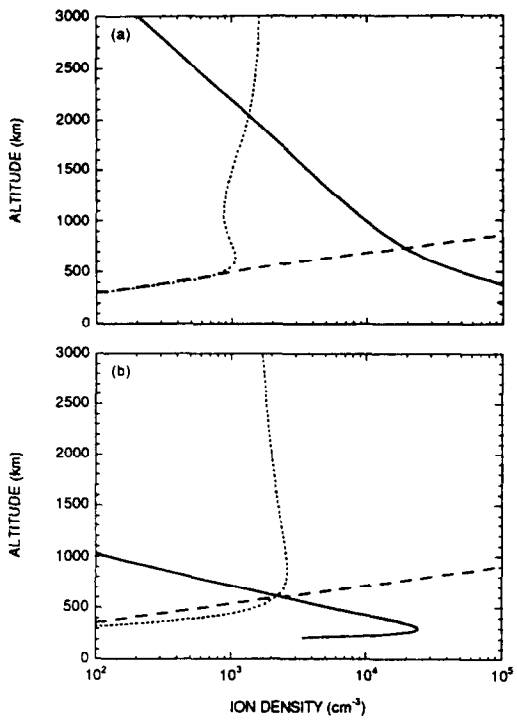

Fig. 3. Profiles of O^+ (——) and (– – – –) during summer at $L = 2$; (a) 12:00 L.T. and (b) 24:00 L.T. Chemical equilibrium levels of H^+ (— — —) are also shown

This implies that "full" plasmaspheric densities during the daytime can be substantially smaller than saturation levels (the winter daytime profiles also indicate significant upgoing fluxes). Ionospheric signatures of this have been observed by Raitt and Dorling (1976).

Saturation levels in the ionosphere can be estimated from the density, n_{tc} at the location where the H^+ chemical equilibrium profile crosses the O^+ profile. Peak saturation levels in the ionosphere are somewhat smaller (but of the same order) as n_{tc}. Thus, H^+ ionospheric densities at 12:00 L.T. (Fig. 3a) are roughly a factor of 10 smaller than saturation levels. Night-time densities, on the other hand (see Fig. 3b), are somewhat larger than saturation levels. This is evident from the fact that H^+ levels are larger than chemical equilibrium values (below 500 km), and is due to a downward flux of ions supplied by the plasmasphere.

While saturation levels [required to obtain the ionosphere–magnetosphere coupling fluxes in equation (18)] can be estimated from equation (15), this is not done here for two reasons. First, plasmaspheric densities tend to be overestimated when calculated using O^+ densities obtained from the IRI empirical ionosphere. Using a time-dependent, hydrodynamic model of the plasmasphere, Rasmussen and Schunk (1990) found that the numerical model overestimated maximum plasmaspheric densities, usually by a factor of approximately 2. Krinberg and Tashchilin (1982) overestimated plasmaspheric densities by a factor of 3–4 using an analytical model similar to equation (15). Although their model overestimated plasmaspheric densities, they found that it gave the correct variation with L-shell. This fact will be exploited below.

The second reason for not employing equation (15) directly is that time scales for refilling the plasmasphere [see equation (19)] are likely to be different from time scales for emptying the plasmasphere. Richards and Torr (1985) showed that refilling depends primarily on the rate at which H^+ is produced in the upper ionosphere and not on H^+ diffusion rates. However, H^+ loss rates are very low at high altitudes and, in order for H^+ to be lost via charge exchange with atomic oxygen, it must first diffuse through an increasingly dense region of O^+. Thus, plasmaspheric loss rates must depend on the coefficient of diffusion, and time scales for plasmaspheric emptying will be, in general, different from time scales for refilling.

In what follows in the next section, we assume that plasmaspheric densities approach equilibrium at a rate given by the time scale in equation (19), but where n_0 is no longer the instantaneous saturation density. Instead, at low L-shells, we obtain n_0 from an empirical model of the full plasmasphere (Carpenter and Anderson, 1992). For $L > 3$, densities obtained from the empirical model at $L = 3$ are scaled to higher L-shells by assuming that ionospheric saturation levels are independent of L and using equation (17) to obtain the density distribution along B. This is done because the plasmasphere at higher L-shells is seldom entirely full, due to the relatively long period of time for refilling compared to the frequency of substorms (which deplete the plasmasphere).

How well does the simple model of plasmaspheric density we have presented here work? Assuming no perpendicular transport, a constant saturation density, n_0 and a diurnally averaged time constant, τ_a, equations (6) and (18) lead to:

$$\frac{\partial \bar{n}}{\partial t} = \frac{n_0 - \bar{n}}{\tau_a}. \tag{21}$$

Assuming that the plasmasphere is totally depleted at time $t = 0$, equation (21) has the analytical solution:

$$\bar{n}(t) = n_0(1 - e^{-t/\tau_a}). \tag{22}$$

A comparison between this simple model of the plasmasphere and the numerical, first-principles model (Guiter *et al.*, 1991) is shown in Fig. 4, where the *solid curve* depicts the results of the numerical model for the first 13 days of refilling. The numerical model was not run for a longer period of time than this because it requires a

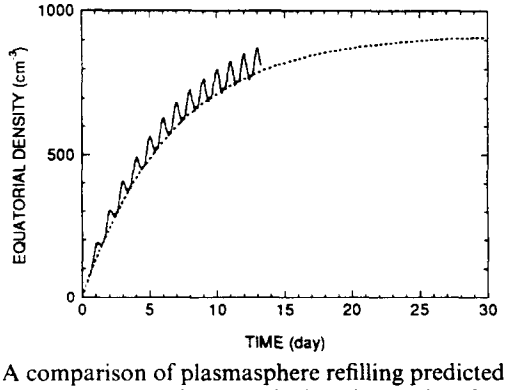

Fig. 4. A comparison of plasmasphere refilling predicted by two different models. The *solid curve* depicts the results of a numerical model and the *dashed curve* is a solution to equation (22) with $n_0 = 920\ \text{cm}^{-3}$ and $\tau_a = 6.7$ days

significant amount of computer resources to run. The dashed curve in the figure was obtained from equation (22) with a saturation density of $n_0 = 920$ cm^{-3} and a time constant of $\tau_a = 6.7$ days. The saturation density was obtained by first estimating its value and then using the numerical model to refine the estimate. n_0 was chosen at a local time of 24:00. The value of the refilling time constant was chosen to best fit the results of the numerical model.

There is a very close correspondence between the two curves in Fig. 4, although there is a diurnal variation in the numerical results which is not seen in the simple model. As the sun rises and heats the plasmasphere, density levels predicted by the numerical model increase above those predicted by the simple model, but by 24:00 L.T. each day, the equatorial plasma density has fallen again and the predictions of the two models are very similar. The close agreement between the two models implies that equation (18) is a good approximation for the time dependence of the refilling fluxes.

In summary, the plasmaspheric model is conceptually very simple. At any given time, the average density in a flux tube depends on only three things: (1) the average density at a previous time; (2) the effects of a change in flux tube volume as a plasma element drifts across L-shells; and (3) the contribution of flux flowing into or out of conjugate ionospheres. The major assumptions of this model are that the average density in a flux tube is approximately equal to the plasma density near the equatorial plane, and that the contribution of the ionosphere behaves according to equation (18). We believe that modeled densities are accurate to within roughly a factor of 2. We test this assumption by comparing with measurements of plasmaspheric density during extended periods of refilling in the next section.

3. Application

Park (1974) has reported plasmaspheric densities during an extended period of time following a magnetic storm which began on 15 June, 1965. As a result of increased magnetospheric convection, the plasmapause moved inward to $L \simeq 2.4$ on 16 June (Carpenter *et al.*, 1971) and refilling began on 17 June as the main phase of the storm ended. The measurements included an eight day period following the end of the storm during which magnetic activity was extremely quiet.

A comparison with these measurements is shown in Fig. 5, where tube content is plotted vs L for selected days during the quiet period following the storm. The solid lines are modeled values and the discrete points are data obtained from whistlers recorded at Eights and at Argentine Islands, Antarctica (Park, 1974). In this figure, N_T is defined as the total number of electrons in a flux tube having 1 cm^2 cross-sectional area at 1000 km altitude and extending to the magnetic equator. Note that this definition differs somewhat from equation (5), particularly in that the integration only extends to the magnetic equator rather than between conjugate ionospheres. The model results were obtained using the empirical plasmaspheric model of Carpenter and Anderson (1992), assuming a plasma temperature $[T_p = (T_i + T_e)/2]$ of 5000K to map empirical densities to L-shells greater than 3, as described above. Additional parameters included a sunspot number $Rs = 20$, $Ap = 10$ and a geographic longitude of 270°. The IRI empirical model was used for ionospheric quantities and MSIS-86 for neutral quantities.

By the eighth day following the end of the storm, the plasmasphere had completely filled to an L of about 4. In the top panel of Fig. 5, it is seen that the model correctly predicts the saturated levels. Beyond $L = 4$, however, the model somewhat overestimates tube content. This occurred because average refilling fluxes obtained from equation (18) were larger than actual fluxes during the first four days of refilling. This can be seen in the bottom two panels of the figure, where modeled densities are roughly a factor of 2 higher than the observations for $L > 4$. As reported by Park (1974), refilling fluxes increased substantially during the fourth day of refilling and, thus, the modeled densities in the top two panels are much closer to the observations beyond an L of 4 than in the lower two panels.

The empirical model of Carpenter and Anderson (1992) predicts plasmaspheric density as a function of L-shell, day of the year and solar activity. In Fig. 6, we vary these parameters in order to estimate refilling times for solar minimum and maximum conditions, as well as for June (*solid lines*) and December (*dashed lines*) solstices. The refilling times plotted in the figure assume that magneto-

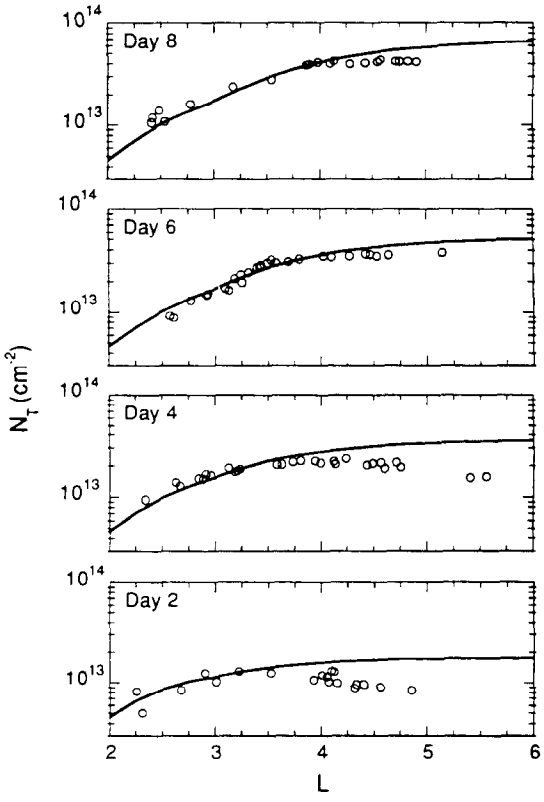

Fig. 5. Recovery of the plasmasphere following a geomagnetic storm. Tube content predicted by the model (——) is compared with the observations of Park (1974) (○) as a function of L, for selected days following the beginning of the quiet period

spheric convection is such that the plasmapause will form beyond $L = 6$. This obviously will not occur under all circumstances. The most striking point suggested by these results is the very long time it takes to refill the plasmasphere at higher L-shells. This is due to the L^4 dependence of flux tube volume. By comparison, saturation densities decrease relatively slowly with L, while refilling fluxes are nearly constant.

Long refilling times are especially evident during solar maximum, when the plasmasphere takes over 150 days to refill at $L = 6$. The long refilling times imply that during solar maximum, the plasmasphere is never likely to be entirely filled beyond an L of about 3. By comparison, during solar minimum the plasmasphere may at times become saturated up to an L of approximately 4 (as was seen in Fig. 5). The dependence of refilling time on solar activity is primarily due to a decrease in atomic hydrogen in the upper ionosphere as solar activity increases. As pointed out by Richards and Torr (1985), the limiting H^+ flux F_1 [see equation (20)] depends sensitively on atomic hydrogen levels. During solar maximum, lower levels of atomic hydrogen imply lower rates of H^+ production, lower limiting fluxes and, ultimately, longer refilling times.

An annual variation in the time it takes for the plasmasphere to refill is also noted in Fig. 6. Below $L = 3$ at solar maximum, refilling takes longer during December (*dashed line*) than during June (*solid line*). This is due primarily to higher plasmaspheric levels predicted by the empirical model during December. For instance, at $L = 2.25$, saturated densities are a factor of 1.8 times higher during December than during June. At higher L-values this ratio decreases, so the annual variation in refilling times seen in Fig. 6 for $L > 4$ is primarily due to annual variations in parameters affecting limiting H^+ fluxes. It should be noted that observations of annual variations in plasmaspheric density have been discussed previously by Park *et al.* (1978) and more recently by Clilverd *et al.* (1991 and references therein).

Refilling times beyond $L = 3$ in Fig. 6 should probably be regarded as an upper limit. Recall that saturation densities for $L > 3$ were scaled according to the L-dependence in equation (17). This implies a constant (with L) saturation density at the ionosphere, with variations in plasmasphere equatorial density occurring only as a result

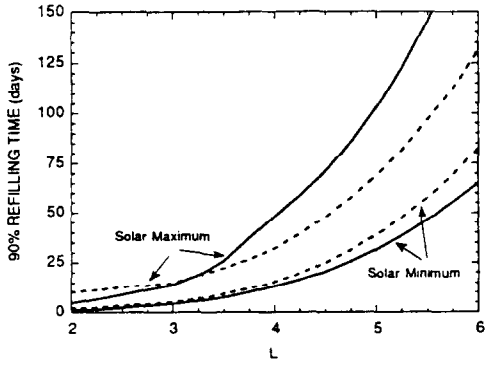

Fig. 6. Modeled refilling times as a function of L for solar maximum and minimum conditions and for June (——) and December (– – – –) solstices

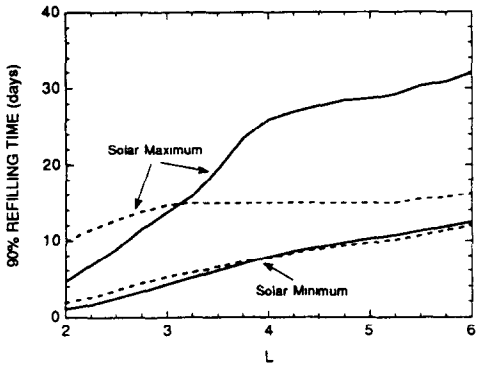

Fig. 7. Modeled refilling times as a function of L for solar maximum and minimum conditions and for June (——) and December (– – – –) solstices. Similar to Fig. 5 except that plasmaspheric equilibrium densities were obtained from Carpenter and Anderson (1992) to an L of 5.2, with an L^{-3} variation assumed thereafter

of an increase in equatorial altitude with increasing L. However, H^+ saturation levels are proportional to the ionospheric O^+ density [see equation (16)]. Thus, as ionospheric O^+ varies, so must plasmaspheric saturation levels. For instance, substantially reduced O^+ levels occur in the main midlatitude trough at night-time (e.g. Muldrew, 1965). The location of the ionospheric trough varies with magnetic activity, but it is nominally located between 60° and 65° invariant latitude. It is expected that plasmaspheric saturation levels would be substantially reduced in the vicinity of the midlatitude trough and that refilling times would be correspondingly smaller.

A lower limit for refilling times has been obtained by assuming that the empirical model of Carpenter and Anderson (1992) represents a completely full plasmasphere out to an L of 5.2; beyond $L = 5.2$, a density variation of L^{-3} was assumed. Refilling times for this full plasmasphere model are shown in Fig. 7. For $L > 4$, refilling times are substantially reduced from those in Fig. 6. At $L = 5$, for instance, refilling times are roughly a factor of 3 smaller. However, during solar maximum, predicted refilling times are still substantial, with refilling taking approximately 30 days during June at an L of 5. It is emphasized that these values should be regarded as a lower limit, because empirical models are likely to underestimate full plasmaspheric densities at higher L-shells. Refilling times are simply too long at higher L-shells for the plasmasphere ever to be measured in a full state.

4. Summary

The total tube content model of Chen and Wolf (1972) has been extended to model average tube density. It was shown that average tube density is nearly equal to plasmaspheric densities near the equatorial plane of the magnetosphere.

A parametric model of ionosphere–magnetosphere coupling has also been developed. This model is useful in situations where the need for a precise knowledge of the fluxes coupling the ionosphere and magnetosphere is not

sufficient to justify the significant computer costs of a first-principles model. One example where the parametric model can be fruitfully applied is to studies of the evolution of the plasmasphere and the plasmapause during magnetic storms. The reason why the parametric model is particularly useful in plasmaspheric studies is that the time scale for changes in plasmaspheric density as a result of magnetospheric convection is much smaller than the time scale for plasmasphere refilling. Time scales due to convection are of the order of a few hours, while refilling typically takes several days. The philosophy is to accurately track the shorter time scales while approximating the effects of the longer time scales.

It has been assumed that thermal ion fluxes coupling the magnetosphere and the ionosphere decay exponentially with a time scale which depends on ionospheric saturation levels and on the limiting ionospheric flux (i.e. the flux which flows from the ionosphere to the magnetosphere when plasmaspheric levels are near vacuum). The ionosphere becomes saturated when H^+ in the upper ionosphere is in hydrostatic equilibrium with chemical equilibrium levels in the middle ionosphere. It was shown that the H^+ saturation density is proportional to ionospheric O^+ and roughly to the square root of the ratio of atomic hydrogen to atomic oxygen. As O^+ varies during the diurnal cycle, so does the H^+ saturation density. Neither the plasmasphere nor the ionosphere can immediately respond to changes in the saturation level, but the two regions attempt to do so via coupling fluxes. Even at an L of 2, the plasmasphere is never in equilibrium with ionospheric saturation levels, because the plasmasphere cannot fill enough during the day to compensate for the reduction in density that occurs during the night.

The parametric model of ionosphere–magnetosphere coupling fluxes has been compared with whistler measurements of plasmaspheric density, observed during an extended period of time following a magnetic storm (Park, 1974). The model predicted refilling fluxes somewhat higher than observed fluxes during the first few days' refilling. On the fourth day of the magnetically quiet period, observed fluxes were higher than the predicted values, while on subsequent days the observed and predicted fluxes were comparable. Predicted densities were within a factor of 2 of the observed values at all times.

The length of time it takes to refill the plasmasphere has also been examined. Substantial differences (a factor of 3–4) in refilling times were noted between solar minimum and solar maximum conditions. Refilling at solar maximum requires a longer period of time, primarily because of lower values of atomic hydrogen in the upper ionosphere, although plasmaspheric equilibrium levels are also somewhat higher during solar maximum. Predicted refilling times depend on the equilibrium plasmaspheric model used, with refilling times varying from a lower limit of the order of 30 days to as high as 100 days at $L = 5$ during June, solar maximum. Refilling time scales also depend on the month of the year. At June solstice and solar maximum, refilling is predicted to require a shorter period of time for $L < 3.2$ and a longer period for $L > 3.2$.

Acknowledgements. This work was supported by the National Aeronautics and Space Administration under grant NAGW-2162 and the National Science Foundation grant ATM-9116858. One of us (SMG) was supported by NASA Marshall Space Flight Center through the graduate student training grant NGT-50368. Acknowledgment is also made to the National Center for Atmospheric Research, sponsored by the National Science Foundation, for computing time used in this research.

References

Bilitza, D., International Reference Ionosphere: recent developments. *Radio Sci.* **21**, 343, 1986.

Binsack, J. H., Plasmapause observations with the M.I.T. experiment on *Imp* 2. *J. geophys. Res.* **72**, 5231, 1967.

Carpenter, D. L., Whistler studies of the plasmapause in the magnetosphere. *J. geophys. Res.* **71**, 693, 1966.

Carpenter, D. L. and Anderson, R. R., An *ISEE*/whistler model of equatorial electron density in the magnetosphere. *J. geophys. Res.* **97**, 1097, 1992.

Carpenter, D. L., Parks, C. G., Arens, J. F. and Williams, D. J., Position of the plasmapause during a stormtime increase in trapped energetic ($E > 280$ keV) electrons. *J. geophys. Res.* **76**, 4669, 1971.

Chappell, C. R., Recent satellite measurements of the morphology and dynamics of the plasmasphere. *Rev. Geophys. Space Phys.* **10**, 951, 1972.

Chappell, C. R., Detached plasma regions in the magnetosphere. *J. geophys. Res.* **79**, 1861, 1974.

Chen, A. J. and Wolf, R. A., Effects on the plasmasphere of a time-varying convection electric field. *Planet. Space Sci.* **20**, 483, 1972.

Clilverd, M. A., Smith, A. J. and Thomson, N. R., The annual variation in quiet time plasmaspheric electron density, determined from whistler mode group delays. *Planet. Space Sci.* **39**, 1059, 1991.

Gombosi, T. I. and Rasmussen, C. E., Transport of gyration-dominated plasmas of thermal origin 1. Generalized transport equations. *J. geophys. Res.* **96**, 7759, 1991.

Guiter, S. M., Gombosi, T. I. and Rasmussen, C. E., Diurnal variations on a plasmaspheric flux tube: light ion flows and *F*-region temperature enhancements. *Geophys. Res. Lett.* **18**, 813, 1991.

Hedin, A. E., MSIS-86 thermospheric model. *J. geophys. Res.* **92**, 4649, 1987.

Ho, D. and Carpenter, D. L., Outlying plasmasphere structure detected by whistlers. *Planet. Space Sci.* **24**, 987, 1976.

Krinberg, I. A. and Tashchilin, A. V., Refilling of geomagnetic force tubes with a thermal plasma after magnetic disturbance. *Ann. Geophys.* **38**, 25, 1982.

Li, W., Sojka, J. J. and Raitt, W. J., A study of plasmaspheric density distributions for diffusive equilibrium conditions. *Planet. Space Sci.* **31**, 1315, 1983.

Maynard, N. C. and Grebowsky, J. M., The plasmapause revisited. *J. geophys. Res.* **82**, 1591, 1977.

Muldrew, D. B., *F*-layer ionization troughs deduced from *Alouette* data. *J. geophys. Res.* **70**, 2635, 1965.

Moffett, R. J., Bailey, G. J., Quegan, S., Rippeth, Y., Samson, A. M. and Sellek, R., Modelling the ionospheric and plasmaspheric plasma. *Phil. Trans. R. Soc. Lond.* **A328**, 255, 1989.

Murphy, J. A., Bailey, G. J. and Moffett, R. J., A theoretical study of the effects of quiet-time electromagnetic drifts on the behavior of thermal plasma at mid-latitudes. *J. geophys. Res.* **85**, 1979, 1980.

Park, C. G., Some features of plasma distribution in the plasmasphere deduced from Antarctic whistlers. *J. geophys. Res.* **79**, 169, 1974.

Park, C. G., Carpenter, D. L. and Wiggin, D. B., Electron density in the plasmasphere: whistler data on solar cycle, annual, and diurnal variations. *J. geophys. Res.* **83**, 3137, 1978.

Raitt, W. J. and Dorling, E. B., The global morphology of light

ions measured by the *ESRO-4* satellite. *J. atmos. terr. Phys.* **38**, 1077, 1976.

Rasmussen, C. E. and Schunk, R. W., A three-dimensional time-dependent model of the plasmasphere. *J. geophys. Res.* **95**, 6133, 1990.

Richards, P. G. and Torr, D. G., Seasonal, diurnal and solar cyclical variations of the limiting H^+ flux in the Earth's topside ionosphere. *J. geophys. Res.* **90**, 5261, 1985.

Rishbeth, H. and Garriott, O. K., *Introduction to Ionospheric Physics*, p. 153. Academic Press, New York, 1969.

Singh, N., Role of ion temperature anisotropy in multistage refilling of the outer plasmasphere. *Geophys. Res. Lett.* **18**, 817, 1991.

Taylor, H. A. Jr, Brinton, H. C. and Pharo, M. W. III, Contraction of the plasmasphere during geomagnetically disturbed periods. *J. geophys. Res.* **73**, 961, 1968.

Appendix: Dipole coordinate system

Useful parameters associated with a dipole coordinate system are provided. The coordinate system considered here is similar to that of Murphy *et al.* (1980). First, a description of some of the symbols used is given:

r, θ, ϕ	radius, colatitude, azimuthal angle
ϕ, q, s	dipole coordinates (right-handed system)
h_ϕ, h_q, h_s	coordinate scale factors
B	magnetic field
χ	angle of magnetic field from horizontal
V	tube volume per unit magnetic flux
R_E	Earth radius
L	McIlwain parameter

The magnetic field is:

$$B = \frac{B_0}{(r/r_0)^3}\sqrt{1+3\cos^2\theta}, \tag{A1}$$

where B_0 is the equatorial value of the magnetic field at the reference altitude r_0. The volume of a flux tube is:

$$V = \frac{32 r_0 L^4}{35 B_0}\sqrt{1-L^{-1}}\,(1+\tfrac{1}{2}L^{-1}+\tfrac{3}{8}L^{-2}+\tfrac{5}{16}L^{-3}). \tag{A2}$$

Orthogonal curvilinear coordinates are:

azimuthal angle, ϕ,

$$q = \left(\frac{R_E}{r}\right)\sin^2(\theta) \tag{A3}$$

and:

$$s = \left(\frac{R_E}{r}\right)^2\cos(\theta), \tag{A4}$$

where s is aligned with, and q is perpendicular to, the magnetic field.

Unit vectors are:

$$\hat{\mathbf{e}}_\phi = -\sin(\phi)\hat{\mathbf{e}}_x + \cos(\phi)\hat{\mathbf{e}}_y, \tag{A5}$$

$$\hat{\mathbf{e}}_q = -\cos(\chi)\hat{\mathbf{e}}_r + \sin(\chi)\hat{\mathbf{e}}_\theta, \tag{A6}$$

and

$$\hat{\mathbf{e}}_s = -\sin(\chi)\hat{\mathbf{e}}_r - \cos(\chi)\hat{\mathbf{e}}_\theta, \tag{A7}$$

where:

$$\hat{\mathbf{e}}_r = \sin(\theta)[\cos(\phi)\hat{\mathbf{e}}_x + \sin(\phi)\hat{\mathbf{e}}_y] + \cos(\theta)\hat{\mathbf{e}}_z \tag{A8}$$

and:

$$\hat{\mathbf{e}}_\theta = \cos(\theta)[\cos(\phi)\hat{\mathbf{e}}_x + \sin(\phi)\hat{\mathbf{e}}_y] - \sin(\theta)\hat{\mathbf{e}}_z. \tag{A9}$$

Scale factors are:

$$h_\phi = r\sin(\theta), \tag{A10}$$

$$h_q = rL\cos(\chi) = \frac{R_E}{\sin(\theta)\sqrt{1+3\cos^2\theta}}\left(\frac{r}{R_E}\right)^2 \tag{A11}$$

and:

$$h_s = \frac{R_E B_0}{B} = \frac{R_E}{\sqrt{1+3\cos^2\theta}}\left(\frac{r}{R_E}\right)^3. \tag{A12}$$

An element of arc length along a field line is:

$$ds_a = h_s\,ds = \frac{-1}{\sin(\chi)}\,dr = -R_E L\sin(\theta)\sqrt{1+3\cos^2\theta}\,d\theta, \tag{A13}$$

where:

$$ds = -\left(\frac{R_E}{r}\right)^2\frac{\sqrt{1+3\cos^2\theta}}{\cos(\chi)}\,d\theta = -\left(\frac{R_E}{r}\right)^3\frac{\sqrt{1+3\cos^2\theta}}{R_E\sin(\chi)}\,dr \tag{A14}$$

and:

$$d\theta = \frac{\tan(\theta)}{2r}\,dr. \tag{A15}$$

Useful transformations:

$$L = \frac{r}{R_E\sin^2\theta}, \tag{A16}$$

$$\cos(\chi) = \frac{\sin\theta}{\sqrt{1+3\cos^2\theta}}, \tag{A17}$$

$$\sin(\chi) = \frac{2\cos\theta}{\sqrt{1+3\cos^2\theta}}, \tag{A18}$$

$$\tan(\chi) = 2\cot(\theta), \tag{A19}$$

$$\sqrt{1+3\cos^2\theta} = 2\sqrt{1+\tfrac{3}{4}\sin^2\theta} = 2\sqrt{1-\frac{3r}{4R_E L}}, \tag{A20}$$

$$\frac{d\theta}{dt} = \frac{-\sin(\chi)\cos(\chi)}{L}\frac{dL}{dt}, \tag{A21}$$

$$\frac{dr}{dt} = \frac{r\cos^2(\chi)}{L}\frac{dL}{dt}, \tag{A22}$$

and:

$$\frac{dL}{dt} = \frac{v_{eq}}{R_E}, \tag{A23}$$

where v_{eq} is the magnetospheric convection velocity in the equatorial plane.

Derivatives:

$$\frac{\partial}{\partial q} = -h_q\left(\cos(\chi)\frac{\partial}{\partial r} - \frac{\sin(\chi)}{r}\frac{\partial}{\partial\theta}\right) \tag{A24}$$

and:

$$\frac{\partial}{\partial s} = -h_s\left(\sin(\chi)\frac{\partial}{\partial r} + \frac{\cos(\chi)}{r}\frac{\partial}{\partial\theta}\right). \tag{A25}$$